Bone Research (2013) 4: 355-361.
www.boneresearch.org

ORIGINAL ARTICLE

Elevated Intracellular Ca^{2+} Signals by Oxidative Stress Activate Connexin 43 Hemichannels in Osteocytes

Manuel A. Riquelme, Jean X. Jiang*

Department of Biochemistry, the University of Texas Health Science Center San Antonio, San Antonio, Texas 78229-3900, USA

Elevated oxidative stress (OS) during aging leads to bone loss. OS increases intracellular Ca^{2+} ($[Ca^{2+}]_i$), resulting in cellular damage and death. We show earlier that Cx43 hemichannels open in response to OS, which serves as a protective mechanism for osteocytes. However, the underlying mechanism is unknown. Here, we found that treatment with H_2O_2 increased $[Ca^{2+}]_i$ in osteocytes with $[Ca^{2+}]_i$ being primarily derived from an extracellular Ca^{2+} source. Hemichannel opening induced by OS was inhibited by the depletion of $[Ca^{2+}]_i$ with BAPTA-AM, a Ca^{2+} chelator, suggesting that $[Ca^{2+}]_i$ influenced the activity of Cx43 hemichannels. Conversely, blockade of hemichannels had no effect on $[Ca^{2+}]_i$. A biotinylation assay showed that cell surface-expressed Cx43 was increased by OS, which could be inhibited by BAPTA-AM, suggesting that $[Ca^{2+}]_i$ is necessary for Cx43 migration to the cell surface in response to OS. Together, these data suggest that increased hemichannel activity induced by OS was likely to be caused by elevated $[Ca^{2+}]_i$ through increased Cx43 on the cell surface.

***Keywords*:** connexin hemichannels; calcium; osteocytes

Bone Research (2013) **4**: 355-361. doi: 10.4248/BR201304006

Introduction

Osteocytes, comprising of approximately 95% of all bone cells, are embedded inside of the bone matrix. Their long dendritic processes form a communication network between neighboring osteocytes and with cells on the bone surface to regulate bone remodeling. During aging, the number of viable osteocytes decreases gradually (1). Oxidative stress (OS) is thought to be a major factor attributing to osteocyte apoptosis and subsequent bone loss (2).

In oxidation-related cellular damage, an increase in the intracellular Ca^{2+} ($[Ca^{2+}]_i$) concentration is known to accelerate damage to osteocyte by activating Ca^{2+}-dependent proteases, although cellular Ca^{2+} overload may not be the sole mechanism mediating cell death (3). Some possible mechanisms by which oxygen radicals cause $[Ca^{2+}]_i$ elevation in different cell types have been reported. Oxygen radicals are shown to induce Ca^{2+} release from intracellular Ca^{2+} stores in hippocampal neurons (4). In human neutrophils, oxygen radicals induce Ca^{2+} influx from the extracellular space (5). Moreover, oxygen radicals are shown to be responsible for Ca^{2+}-dependent mitochondrial dysfunction and Ca^{2+} entry (6). However, the precise mechanisms of H_2O_2-induced $[Ca^{2+}]_i$ elevation remain largely unknown.

Connexin (Cx) molecules form both gap junctions and hemichannels, of which the former mediates inter-cellular communications between cells and the latter mediates the communication between the intracellular and extracellular environments. These channels permit

*Correspondence: Jean X. Jiang
E-mail: jiangj@uthscsa.edu
Tel: 210 567 3796; Fax: 210 567 6318
Received 25 September 2013; Accepted 27 October 2013

the exchange of small molecules (up to ~1 kDa) (7). Hemichannels are formed by 6 Cx proteins. Cx43 is the major connexin isoform expressed in bone cells and the activity of hemichannels induced by OS is primarily mediated by Cx43 hemichannels (8). Cx43 hemichannels have been shown to regulate the release of NAD^+, prostaglandin E_2 (PGE_2), and ATP in response to mechanical stimulation in osteocytes (8). Cx43 plays a critical role in many aspects of bone cell function, including proliferation, survival, and differentiation of osteoblasts, skeletal development, and postnatal bone mass acquisition (9-10). Furthermore, Cx43 is shown to be required for the anti-apoptotic effect of bisphosphonates on osteoblasts and osteocytes in vivo (11). However, the cellular mechanism that regulates the activity of Cx43 hemichannels by OS is poorly understood. In this study, we uncovered the role of intracellular Ca^{2+} rise induced by OS in the regulation of Cx43 hemichannels. These findings will ultimately help to illustrate the underlying mechanism of Cx43 hemichannel opening and OS-induced Ca^{2+} signals in osteocytic cell death and bone aging.

Materials and Methods

Materials

Fetal bovine serum (FBS) and calf serum (CS) were from HyClone Laboratories (Logan, UT, USA); rat tail collagen type I, 99% pure, was from Becton Dickinson Laboratories (Bedford, MA, USA); Fluo-4 AM were from Invitrogen (Eugene, OR, USA); EZ-link Sulfo-NHS-LC-Biotin and NeutrAvidine from Pierce Biotechnology (Rockford, IL, USA); paraformaldehyde (16% stock solution) was from Electron Microscopy Science (Fort Washington, PA, USA); nitrocellulose membrane was from Schleicher & Schuell (Keene, NH, USA); Enhanced Chemiluminescence (ECL) kit was from Amersham Biosciences (Piscataway, NJ, USA); X-OMAT AR films were from Eastman Kodak (Rochester, NY, USA). All other chemicals were from either Sigma (St. Louis, MO, USA) or Fisher Scientific (Pittsburgh, PA, USA).

Cell culture

MLO-Y4 cells were cultured on collagen-coated (rat tail collagen type I; 0.15 $mg \cdot mL^{-1}$) surfaces. Cells were grown in α-modified essential medium (MEM) supplemented with 2.5% FBS and 2.5% CS, and incubated in a 5% CO_2 incubator at 37 ℃ as described previously (12).

Time-lapse fluorescence imaging and [Ca2+]i

$[Ca^{2+}]_i$ changes were monitored in MLO-Y4 cells plated on collagen coated glass bottom cell culture plate (MatTek, Ashland, MA, USA). Cells were ester-loaded with 5 $\mu mol \cdot L^{-1}$ Fluo-4 for 45 min at 37 ℃ and then washed three times in recording medium. Cells were maintained for another 5 min at 37 ℃ before any fluorescence recording was performed. The Ca^{2+} imaging was acquired every 30 s during 100 min using a 20× dry objective at 37 ℃ in an inverted microscope (Nikon Eclipse) with a fluorescein filter. The image analysis was performed with Image J software by measuring an average of pixel density of 15 random cells and subtracting the background fluorescence. The average pixel value allocated to each cell was corrected for background. Because of low excitation intensity, no bleaching was observed even illuminating the cells over a few minutes. The ΔF ratio was obtained by first subtracting fluorescence during the rest (F_0) and the fluorescence at the time of recording (F), and then dividing by F_0 on the pixel-by-pixel base [$\Delta F=(F-F_0)/F_0$]. This average value was subtracted by basal, non-stimulated signal to correct the photo-bleaching effect due to the recording.

Dye uptake

MLO-Y4 cells were plated onto 35 mm cell culture dish for 48 h to reach 70% of confluence. Then cells were incubated in absence or presence of 5 $\mu mol \cdot L^{-1}$ BAPTA-AM and then were rinsed 3 times with 2 mL of recording medium (HCO_3^- -free α-MEM with 10 $mmol \cdot L^{-1}$ HEPES). The cells were treated for 30 min with 0.3 $mmol \cdot L^{-1}$ H_2O_2 and then were exposed to 2 mL recording medium with 50 $\mu mol \cdot L^{-1}$ ethidium bromide (EtBr) and fluorescein dextran (~10 kDa) for 5 min. Dropping assay was performed to serve as a control for the hemichannel activity. Cell culture dishes were divided in 8 areas and 200 µL of recording media were dropped on top of the cell in the presence of EtBr. After the dropping was finished, the cells were incubated in the presence of the dye for 5 min and were then rinsed 3 times with PBS and fixed with 2% formaldehyde. At least 4 microphotographies of fluorescence fields were taken with a 10X dry objective in an inverted microscope (Carl Zeiss) with a rhodamine filter for EtBr and fluorescein filter for fluorescein dextran. The image analysis was performed with Image J software by measuring the average of pixel density of 15 random cells and subtracting the background fluorescence.

Immunoblots

MLO-Y4 cells were seeded at $3x10^5$ per 60 mm dishes for 48 h, rinsed twice with cold PBS, and harvested by scraping with a rubber policeman on ice in 200 µL of Laemmli sample buffer containing protease and phosphatase inhibitors. Cell lysates were analyzed by immunoblotting.

Briefly, 20 μL cell lysates were separated on 10% SDS-PAGE and electro-transferred to nitrocellulose sheets. Nonspecific protein binding was blocked by incubation of nitrocellulose sheets in 10% nonfat milk for 30 min, and then blots were incubated with an affinity-purified polyclonal anti-Cx43 antibody (1:300 dilution in PBS containing 2% nonfat milk) overnight at 4 ℃, followed by six, 10 min each washes with PBS containing 0.5% Tween-20. Blots were incubated with goat anti-rabbit secondary antibody conjugated to horseradish peroxidase (1:2 500 in PBS containing 2% nonfat milk). Antigen-antibody complexes were detected by ECL using the SuperSignal kit according to the manufacturer's instructions. Resulting immunoblot signals were scanned and densitometric analyses were performed using the Image J software.

Surface protein biotinylation

Cell cultures seeded in 60 mm culture dishes were washed three times with DPBS containing 1 mmol·L^{-1} $CaCl_2$ and 1 mmol·L^{-1} $MgCl_2$ (DPBS-X^{2+}). Then, 2 mL of 0.5 mg·mL^{-1} EZ-link Sulfo-NHS-LC-Biotin (Pierce Biotechnology) (DPBS-X^{2+}) was added to each dish and incubated for 30 min at 4 ℃. The cells were washed with DPBS-X^{2+}, and then were incubated with 15 mmol·L^{-1} glycine in DPBS-X^{2+} for 30 min, after which cell lysate was collected in 0.5 mL of radioimmunoprecipitation assay (RIPA) buffer (100 mmol·L^{-1} NaCl, 10 mmol·L^{-1} EDTA, 25 mmol·L^{-1} Tris-HCl, 0.25% Triton X-100, and 1% SDS, pH 7.76) containing protease and phosphatase inhibitors. Cell lysates were then homogenized by passing through a 26-gauge needle syringe 20 times. Total lysates were mixed with 50 mmol·L^{-1} Tris, pH 7.8, to bring the volume to 1 mL, and then incubated with 100 μL of monomeric avidin beads for 1 h at 4 ℃. The beads were then washed with RIPA buffer without SDS, and biotinylated proteins were eluted by boiling the beads for 5 min in sample loading buffer containing 1% SDS and 2% 2-mercaptoethanol, and the eluted proteins were analyzed by Western blotting using an affinity-purified Cx43 antibody. The intensity of Cx43 bands was quantified by densitometry (Image J) and the ratio of biotinylated to total Cx43 was calculated.

Statistical analysis

Data were analyzed using one-way analysis of variance (ANOVA) and the Bonferroni comparison test with the Instat biostatistics program (GraphPad software). Data are presented as the means ± standard errors of the means (SEM) of three determinations. Asterisks indicate the degrees of significant differences compared with the controls (*P<0.05; **P<0.01; ***P<0.001).

Results

OS increases the level of $[Ca^{2+}]_i$ in osteocytes with extracellular Ca^{2+} as a primary source

Intracellular calcium signals were detected by time lapse Ca^{2+} recording in MLO-Y4 cells loaded with Fluo-4 dye. The treatment with 0.3 mmol·L^{-1} H_2O_2 induced a quick and consistent rise of $[Ca^{2+}]_i$ levels (Figure 1A, green line). The depletion of extracellular Ca^{2+} resulted

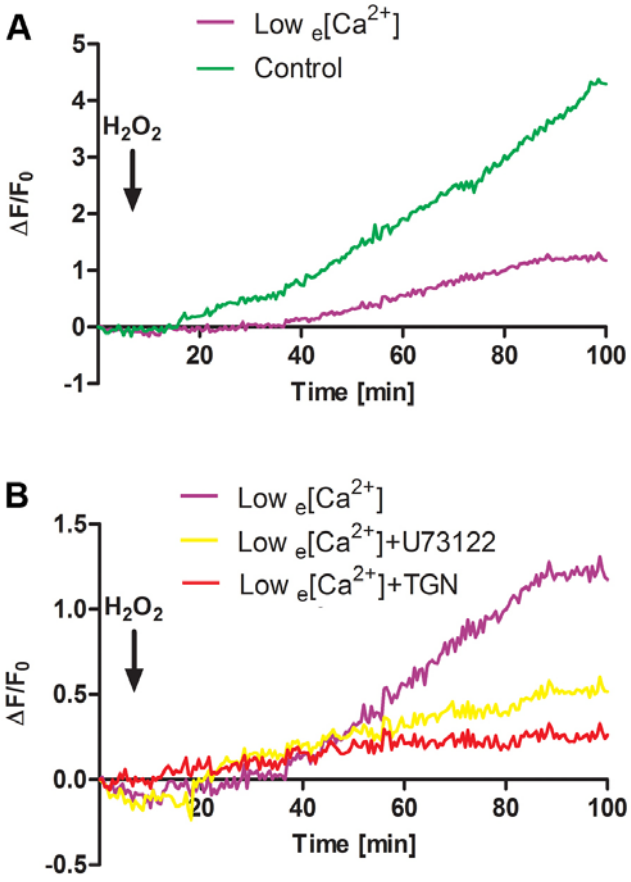

Figure 1 Extracellular Ca^{2+} is a principal source of $[Ca^{2+}]_i$ in osteocytes under OS. (A) MLO-Y4 cells were pre-loaded with 5 μmol·L^{-1} Fluo-4 dye and then treated with 0.3 mmol·L^{-1} H_2O_2 in the presence (control, green line), or absence (low $_e[Ca^{2+}]$, purple line) of extracellular Ca^{2+}. (B) MLO-Y4 cells were pre-loaded with Fluo-4 dye and then pre-treated with 5 μmol·L^{-1} U73122 (yellow line), 0.1 μmol·L^{-1} thapsigargin (TGN, red line) or non-treatment control (purple line) in the absence of extracellular Ca^{2+} prior to the treatment with 0.3 mmol·L^{-1} H_2O_2. Time laps recording of Ca^{2+} signal took place every 30 s during entire 100 min time period. The black arrow indicates the moment when H_2O_2 was added. The lines correspond to an average of 3 independent experiments where 30 cells were quantified and normalized with non-stimulated rest state. The error bars were omitted in order to clearly show the Ca^{2+} signal pattern.

in a reduction of $[Ca^{2+}]_i$ by two-thirds (Figure 1A, purple line), suggesting that the major source of Ca^{2+} was from outside of the cell. To explore the involvement of the intracellular Ca^{2+} stores mediated by the IP_3 pathway and endoplastic reticulum (ER), we used U73122, a phospholipase C (PLC) inhibitor and thapsigargin, an ER Ca^{2+}-ATPase pump inhibitor. In the absence of extracellular Ca^{2+}, both U73221 and thapsigargin dramatically inhibited $[Ca^{2+}]_i$ rise, with more profound effect by thapsigargin. These result suggest that OS increased intracellular Ca^{2+} signals and extracellular Ca^{2+} influx is the major source of $[Ca^{2+}]_i$. Moreover, release of the intracellular store of Ca^{2+} is primarily mediated by PLC-IP_3-mediated Ca^{2+} release from the ER.

Cx43 hemichannel openings in osteocytes are regulated by intracellular Ca^{2+} signals

We have previously shown that Cx43 hemichannel opening is induced by OS and this opening protects osteocytes against OS (8). However, the upstream mechanism that causes the opening of Cx43 hemichannels remains unknown. To determine if elevated $[Ca^{2+}]_i$ induced by OS has any effect on hemichannels, MLO-Y4 cells were treated with or without H_2O_2 and/or the Ca^{2+} chelator, BAPTA-AM, or U73122 (Figure 2A). The treatment with H_2O_2 induced the opening of hemichannels as indicated by the increase of EtBr uptake, with approximately 50% over the basal uptake. The depletion of $[Ca^{2+}]_i$ by a Ca^{2+} chelator or a phospholipase C inhibitor completely prevented the opening of hemichannels induced by OS. To exclude the possibility that BAPTA-AM by itself, but not through the suppression of $[Ca^{2+}]_i$, directly inhibits hemichannel opening, we applied mechanical loading through media dropping to the cell, which has been shown to induce the opening of hemichannels (13). Consistently, media dropping caused an increase of EtBr dye uptake (Figure 2B). Unlike its response to BAPTA-AM under OS, the opening of hemichannels by media dropping was not inhibited by BAPTA-AM. This result excluded the direct effect of BAPTA-AM and support the role of elevated $[Ca^{2+}]_i$ signals on hemichannels. Together, these data suggest that Ca^{2+} signals are an upstream regulator for the opening of hemichannels under OS conditions.

Elevated $[Ca^{2+}]_i$ increases cell surface expression of Cx43

We have previously shown that OS induces a progressive increase of Cx43 protein on the cell surface, reaching the maximum after 1 h (8). To determine if OS-induced $[Ca^{2+}]_i$ rise has any effect on the cell surface expression of Cx43, we treated MLO-Y4 cells with H_2O_2 for 1 h in the absence or presence of BAPTA-AM. The level of Cx43 on the cell surface was then determined by biotinylation and western blotting assays. The treatment of H_2O_2 increased the levels of Cx43 on the cell surface indicated by the increase of biotinylated Cx43 level (Figure 3); however, this increase is reduced by BAPTA-AM (Figure 3). The quantification result of western blots showed that BAPTA-AM significantly attenuated the increase of Cx43 on the cell surface induced by

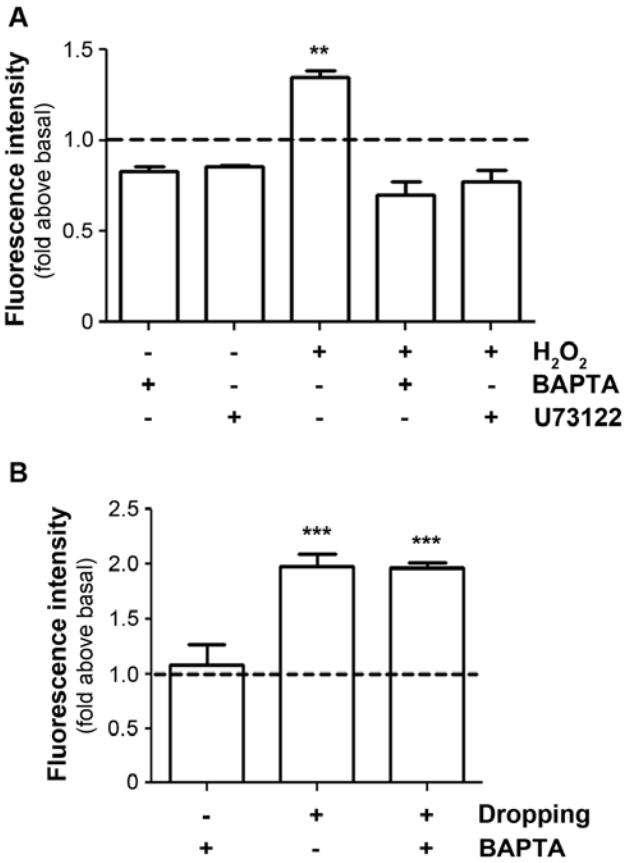

Figure 2 Hemichannels opening induced by OS requires elevated $[Ca^{2+}]_i$. (A) Hemichannel opening induced by H_2O_2 is blocked by depletion of $[Ca^{2+}]_i$. MLO-Y4 cells were pre-incubated with 5 μmol·L^{-1} BAPTA-AM or 5 μmol·L^{-1} U73122 for 20 min and then were incubated with 0.3 mmol·L^{-1} H_2O_2 for 30 min. EtBr dye uptake was performed and imaged by snapshot. The degree of dye uptake was quantified by Image J. The dashed line indicates the normalized basal dye uptake value. H_2O_2 treatment *versus* all other conditions, $^{**}P<0.01$, $n=3$. (B) BAPTA-AM does not block the activation of Cx43 hemichannels induced by media dropping. MLO-Y4 cells were pre-treated with 5 μmol·L^{-1} BAPTA-AM and were stimulated by media dropping to induce Cx43 hemichannels opening. EtBr dye uptake was performed and imaged by snapshot. The degree of dye uptake was quantified by Image J. The dashed line indicates the normalized basal dye uptake value. Non-dropping control with BAPTA-AM *versus* dropping with or without BAPTA-AM, $^{***}P< 0.001$, $n=3$.

H_2O_2 (Figure 3, lower panel). This result suggests that the increased hemichannel activity by OS can be partially explained by the elevated levels of Cx43 on the cell surface, and this process is mediated by the rise of $[Ca^{2+}]_i$.

Cx43 hemichannels have no effect on intracellular Ca^{2+} signals in response to OS

To assess if Cx43 hemichannels would affect OS-induced $[Ca^{2+}]_i$ rise in osteocytes, Fluo-4 dye-loaded MLO-Y4 cells were pre-incubated with or without Cx43 (E2) antibody, a Cx43 hemichannel blocking antibody (14), and were then treated with H_2O_2. The treatment with Cx43 (E2) antibody had a similar OS-induced $[Ca^{2+}]_i$ response as non-treated control (Figure 4). Unlike the role of $[Ca^{2+}]_i$ in Cx43 hemichannels, Cx43 hemichannels are not involved in the generation of intracellular Ca^{2+} signals under OS, which further suggests that $[Ca^{2+}]_i$ is an upstream regulator of Cx43 hemichannels and under OS hemichannels are not responsible for passage of calcium ions.

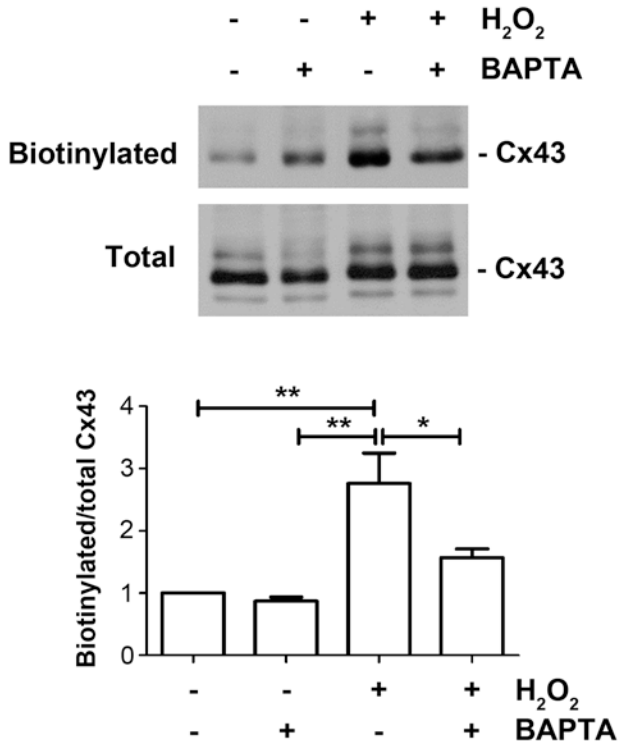

Figure 3 $[Ca^{2+}]_i$ rise induced for OS enhances the levels of Cx43 on the cell surface. MLO-Y4 cells were pre-incubated with 5 μmol·L^{-1} BAPTA-AM, treated with 0.3 mmol·L^{-1} H_2O_2 for 1 h and then were subjected to cell surface biotinylation. Biotinylated samples and total cell lysates were immunoblotted using an affinity purified anti-Cx43 antibody. The band intensity was quantified and the ratio of biotinylated *versus* total Cx43 was calculated (lower panel). **P*<0.05; ***P*<0.01; *n*=3.

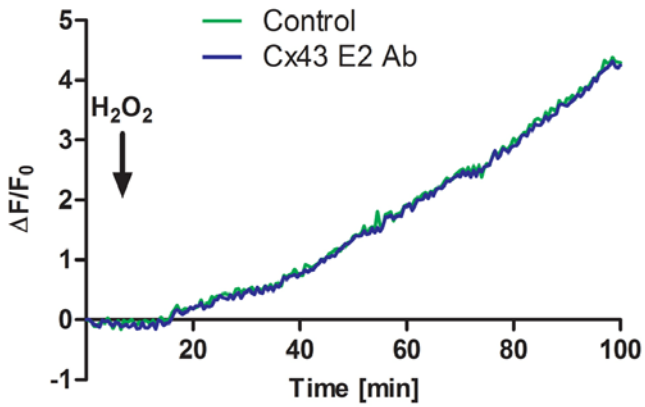

Figure 4 Blockage of Cx43 hemichannels has no effect on elevated $[Ca^{2+}]_i$ induced by OS. MLO-Y4 cells were pre-loaded with Fluo-4 dye and then were treated with 0.3 mmol·L^{-1} H_2O_2 under control (green line) or in the presence of hemichannel-blocking Cx43(E2) antibody (blue line). The black arrow indicates the moment when H_2O_2 was added. The lines correspond to an average of 3 independent experiments where 30 cells were quantified and normalized with non-stimulated rest state. The error bars were omitted in order to clearly illustrate the Ca^{2+} signal pattern.

Discussion

The apoptosis and loss of osteocytes, the most abundant cell type in the bone, are closely associated with skeletal aging and accumulation of reactive oxygen species (2). Osteocytes richly express Cx43, and we have previously shown that Cx43 hemichannels play a critical role in protecting osteocytes against OS (8). However, the underlying regulatory mechanism remained elusive. In this study, as illustrated in Figure 5, we showed that the increased intracellular Ca^{2+} signals activated by OS are a major factor that opens Cx43 hemichannels. The enhancement of hemichannel activities is likely to due to the increased Cx43 levels on the cell surface.

Similar to osteocytes, cells like astrocytes and cardiomyocytes express high levels of Cx43. Under preconditioning conditions induced by OS or ischemia and reperfusion, the presence of Cx43 plays a fundamental role in cell protection. It has been suggested that Cx43 hemichannels release unidentified factors to extracellular media, which activates intracellular signaling pathways involved in cell protection (8, 15-16). However, in other studies, Cx43 hemichannels are indicated to enhance the process of cell death. Cigarette smoke extract, H_2O_2 or OS induced by chemical ischemia, oxygen or glucose deprivation are shown to induce hemichannel opening, which leads to cell death (17-19). Additionally, Cx43 hemichannels cause cadmium-

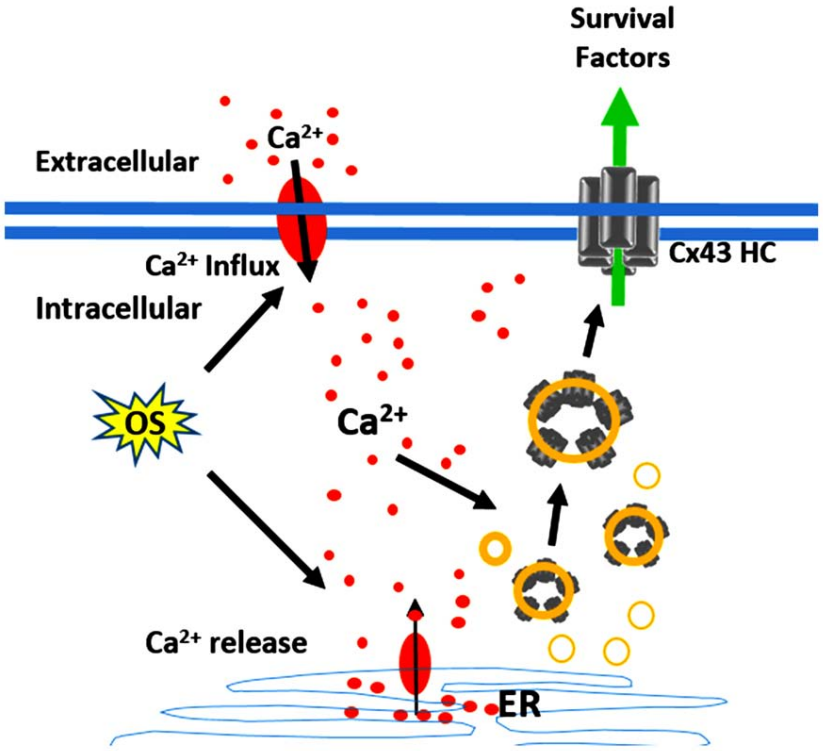

Figure 5 Schematic diagram illustrates the regulation of Cx43 hemichannels by $[Ca^{2+}]_i$ under OS. OS induces $[Ca^{2+}]$ rise as a result of extracellular Ca^{2+} influx and a release of Ca^{2+} from endoplasmic reticulum (ER). Elevated $[Ca^{2+}]$ promotes the increased presence of Cx43 hemichannels (Cx43 HC) on the cell surface.

induced cell death of renal epithelial cells (20). This discrepancy between the roles of Cx43 hemichannel function in cell death versus protection could be caused by the activity and duration of the opening of hemichannels. Sustained opening of hemichannels is known to be detrimental to the cell which depolarizes cell membrane and ultimately leads to cell death. Correspondingly, the prolonged elevation of $[Ca^{2+}]_i$ which sustains the hemichannel opening could be a major mechanism resulting in cell death. Therefore, an intricate balance of Cx43 hemichannel activity is a key factor in deciding cell fate under OS.

$[Ca^{2+}]_i$ rise induced by growth factors or 4-Br-A23187, a slow Ca^{2+} ionophore, has been shown to induce the increase of Cx43 cell surface levels (21). This result is consistent with our observation that increased $[Ca^{2+}]_i$ promotes cell surface expression of Cx43 and the amount of Cx43 increased on the plasma membrane is well correlated with the increased availability of Cx43 in forming functional hemichannels.

Interestingly, we found that the opening of Cx43 hemichannels does not participate in the passage of Ca^{2+} to contribute to total $[Ca^{2+}]_i$ signalling induced by OS. This observation suggests that Ca^{2+} rise in the cytoplasm is possibly attributed by Ca^{2+} influx from outside by high conductance Ca^{2+} channels present on the plasma membrane of osteocytes (22). Additionally, based on our study, release of intracellular stores by PLC-IP_3 signalling also partially contributes to the increase of $[Ca^{2+}]_i$ and Cx43 hemichannel activity in the osteocytes. This data further support the notion that $[Ca^{2+}]_i$ signals are an upstream regulator for the activation of Cx43 hemichannels in osteocytes.

Acknowledgments

We would like Jade Zhou and Danielle Victor for critical reading of the manuscript. The work was supported by Welch Foundation Grant AQ-1507 and National Institutes of Health Grant EY012085 to JXJ.

References

1 Dallas SL, Prideaux M, Bonewald LF. The osteocyte: an endocrine cell and more. Endocr Rev. 2013;34:658-690.

2 Manolagas SC, Parfitt AM. What old means to bone. Trends Endocrinol Metab. 2010;21:369-374.

3 Kikuyama A, Fukuda K, Mori S, Okada M, Yamaguchi H,

Hamanishi C. Hydrogen peroxide induces apoptosis of osteocytes: involvement of calcium ion and caspase activity. Calcif Tissue Int. 2002;71:243-248.

4 Kemmerling U, Muñoz P, Müller M, Sánchez G, Aylwin ML, Klann E, Carrasco MA, Hidalgo C. Calcium release by ryanodine receptors mediates hydrogen peroxide-induced activation of ERK and CREB phosphorylation in N2a cells and hippocampal neurons. Cell Calcium. 2007;41:491-502.

5 Giambelluca MS, Gende OA. Hydrogen peroxide activates calcium influx in human neutrophils. Mol Cell Biochem. 2008;309: 151-156.

6 Feissner RF, Skalska J, Gaum WE, Sheu SS. Crosstalk signaling between mitochondrial Ca2+ and ROS. Front Biosci (Landmark Ed). 2009;14:1197-1218.

7 Goodenough DA, Paul DL. Beyond the gap: functions of unpaired connexon channels. Nat Rev Mol Cell Biol. 2003;4:285-294.

8 Kar R, Riquelme MA, Werner S, Jiang JX. Connexin 43 channels protect osteocytes against oxidative stress-induced cell death. J Bone Miner Res. 2013;28:1611-1621.

9 Stains JP, Civitelli R. Gap junctions in skeletal development and function. Biochim Biophys Acta. 2005;1719:69-81.

10 Batra N, Kar R, Jiang JX. Gap junctions and hemichannels in signal transmission, function and development of bone. Biochim Biophys Acta. 2012;1818:1909-1918.

11 Plotkin LI, Lezcano V, Thostenson J, Weinstein RS, Manolagas SC, Bellido T. Connexin 43 is required for the anti-apoptotic effect of bisphosphonates on osteocytes and osteoblasts in vivo. J Bone Miner Res. 2008;23:1712-1721.

12 Kato Y, Windle JJ, Koop BA, Mundy GR, Bonewald LF. Establishment of an osteocyte-like cell line, MLO-Y4. J Bone Miner Res. 1997;12:2014-2023.

13 Burra S, Nicolella DP, Francis WL, Freitas CJ, Mueschke NJ, Poole K, Jiang JX. Dendritic processes of osteocytes are mechanotransducers that induce the opening of hemichannels. Proc Natl Acad Sci U S A. 2010;107:13648-13653.

14 Siller-Jackson AJ, Burra S, Gu S, Xia X, Bonewald LF, Sprague E, Jiang JX. Adaptation of connexin 43-hemichannel prostaglandin release to mechanical loading. J Biol Chem. 2008;283:26374-26382.

15 Giardina SF, Mikami M, Goubaeva F, Yang J. Connexin 43 confers resistance to hydrogen peroxide-mediated apoptosis. Biochem Biophys Res Commun. 2007;362:747-752.

16 Lin JH, Lou N, Kang N, Takano T, Hu F, Han X, Xu Q, Lovatt D, Torres A, Willecke K, Yang J, Kang J, Nedergaard M. A central role of connexin 43 in hypoxic preconditioning. J Neurosci. 2008; 28:681-695.

17 Ramachandran S, Xie LH, John SA, Subramaniam S, Lal R. A novel role for connexin hemichannel in oxidative stress and smoking-induced cell injury. PLoS One. 2007;2:e712.

18 Contreras JE, Sáez JC, Bukauskas FF, Bennett MV. Gating and regulation of connexin 43 (Cx43) hemichannels. Proc Natl Acad Sci U S A. 2003;100:11388-11393.

19 Orellana JA, Hernández DE, Ezan P, Velarde V, Bennett MV, Giaume C, Sáez JC. Hypoxia in high glucose followed by reoxygenation in normal glucose reduces the viability of cortical astrocytes through increased permeability of connexin 43 hemichannels. Glia. 2010;58:329-343.

20 Fang X, Huang T, Zhu Y, Yan Q, Chi Y, Jiang JX, Wang P, Matsue H, Kitamura M, Yao J. Connexin43 hemichannels contribute to cadmium-induced oxidative stress and cell injury. Antioxid Redox Signal. 2011;14:2427-2439.

21 Schalper KA, Palacios-Prado N, Retamal MA, Shoji KF, Martínez AD, Sáez JC. Connexin hemichannel composition determines the FGF-1-induced membrane permeability and free [Ca2+]i responses. Mol Biol Cell. 2008;19:3501-3513.

22 Thompson WR, Majid AS, Czymmek KJ, Ruff AL, García J, Duncan RL, Farach-Carson MC. Association of the α(2)δ(1) subunit with Ca(v)3.2 enhances membrane expression and regulates mechanically induced ATP release in MLO-Y4 osteocytes. J Bone Miner Res. 2011;26:2125-2139.